A DPIM-based framework for reliability analysis of building structures under stochastic near-fault ground motions

Guohai Chen
Postdoctor, Dept. of Engineering Mechanics, Dalian University of Technology, Dalian, China

Dixiong Yang
Professor, Dept. of Engineering Mechanics, Dalian University of Technology, Dalian, China

ABSTRACT: Near-fault ground motions have the forward directivity effect and fling-step effect, both of which can produce the distinct long-period pulse in velocity time histories. Such velocity pulses with larger amplitude easily result in the nonlinear seismic responses and severe damage to building structures. Generally, earthquake ground motions also possess strong randomness and nonstationary characteristic. Therefore, the stochastic generation model of near-fault ground motions and the reliability assessment of structures play crucial roles in performance-based earthquake engineering. This study proposes the stochastic synthesis model of nonstationary near-fault ground motion and the efficient method for assessing first-passage dynamic reliability for structures. Firstly, the stochastic model for generating stationary near-fault pulse-like ground motions is established. In the model, the velocity time history with the strongest pulse is generated based on the orthogonal horizontal components by using wavelet analysis. The nonstationary model is suggested to synthesize the high-frequency residual acceleration time history. Secondly, the probability density integral equation (PDIE) controlling the propagation of randomness from stochastic ground motions to structural responses is derived based on the principle of probability conservation. By using the techniques of partition of probability space and smoothing of Dirac delta function, the direct probability integral method (DPIM) is proposed to efficiently solve PDIE and obtain the probability density functions of stochastic responses of structures. Moreover, the DPIM is extended to assess the first-passage dynamic reliability of building structures with nonlinear hysteretic behaviour. Finally, the effectiveness of established stochastic model and efficiency of proposed DPIM for seismic reliability assessment for hysteretic frame structure in near-fault area are demonstrated by numerical examples. Additionally, the effect of the velocity pulse on the failure probability of building structures is also scrutinized.

1. INTRODUCTION

Near-fault ground motions are closely related with the rupturing mechanism of the fault, and generally present the effects of forward directivity and fling-step. Both the effects may cause the distinct long-period pulse in velocity time histories (Bray and Rodriguez-Marek 2004). Such velocity pulses possess larger amplitude and long duration and exhibit large uncertainty, which usually result in the nonlinear responses and damage for building structures. Therefore, the reliability assessment of building structures subject to near-fault ground motions is critical for seismic design of structures.

Many studies on the near-fault pulse model have been carried out. Commonly, a simple velocity waveform, such as the trigonometric functions (Mavroeidis and Papageorgiou 2003) and wavelet function (Baker 2007), is used to fit the long-period velocity pulse. Dickinson and Gavin (2011) suggested a statistical analysis method for ground motion records under a seismic hazard level and a geographic region, and obtained the probability distribution of the parameters that describe the low- and high-frequency stochastic contents of ground motions.

By taking the orientation of the strongest pulse into account, Yang and Zhou (2015) proposed a stochastic synthesis model of near-fault pulse-like ground motion, in which the velocity pulse was described by single Gabor wavelet. Dabaghi and Der Kiureghian (2017) suggested another model by combining M-P pulse model and filtered Gaussian random process, which can reflect the nonstationarity of ground motions. In above models, however, a lot of random variables are inevitably introduced to reproduce the near-fault impulsive ground motions. Such models have to make the Monte Carlo simulation (MCS) to assess the dynamic reliability of structures.

Recently, authors proposed an efficient method, namely direct probability integral method (DPIM) (Chen and Yang 2019), for stochastic response analysis of structures. This method is based on the probability density integral equation governing the randomness propagation of structures. With this idea, the DPIM can be easily extended to reliability analysis, including static reliability, dynamic reliability and system reliability (Chen and Yang 2021, Chen et al. 2022). This study aims to evaluate the dynamic reliability of building structures under near-fault ground motions. For this purpose, firstly, this work establishes a stochastic model for near-fault impulsive ground motion, which represented the velocity pulse and time-frequency non-stationarity of near-fault ground motions. Then, the dynamic reliability of building is assessed by utilized the DPIM. Finally, the effects of velocity pulse parameters on dynamic reliability of structures are also scrutinized.

2. STOCHASTIC MODEL OF NEAR-FAULT GROUND MOTIONS

2.1 Long-period velocity pulse

In this paper, the long-period velocity pulse is expressed by the M-P pulse model proposed by Mavroeidis and Papageorgiou (2003) that is

$$V_p(t;T_p,N_c,T_{pk},\varphi) = \frac{PGV}{2}\left[1+\cos\left(\frac{2\pi(t-T_{pk})}{T_pN_c}\right)\right]\cdot\cos\left(2\pi\frac{t-T_{pk}}{T_p}-\varphi\right) \quad (1)$$

where $T_{pk}-T_pN_c/2\le t\le T_{pk}+T_pN_c/2$, and T_p, N_c, T_{pk} and φ represent the pulse period, number of circles in the pulse, the time of peak value of the velocity pulse, respectively; the attenuation of *PGV* is fitted by using the regression formula presented by Bary and Rodriguez-Marekis (2004)

$$\ln\left(PGV\right)=a+bM_w+c\ln(R_{\mathrm{rup}}^2+d^2)+\sigma_{\ln PGV} \quad (2)$$

in which M_w is the moment magnitude; R_{rup} denotes the closest distance from the recording site to the ruptured area, which is considered as the fault distance in this study; and c_1, c_2, c_3 and c_4 are the regression parameters; σ represents the regression residual, respectively.

2.2 High-frequency components

The residual acceleration time series can be generated by extracting the domain pulse and differentiating the residual velocity history. In this study, a random variable based spectral representation method (Liu et al. 2016) is employed to simulate the residual stochastic nonstationary high-frequency components of near-fault ground motion, which is written as

$$a_{\mathrm{res}}(t)=\sum_{k=0}^{N}\sqrt{S(t,\omega_k)\Delta\omega}\cdot\left[\cos(\omega_k t)X_k+\sin(\omega_k t)Y_k\right] \quad (3)$$

where $S(t, \omega_k)$ is the nonstationary power spectral density function of residual acceleration time history; $\Delta\omega=(\omega_u-\omega_l)/N$ denotes the frequency step size; $\omega_k=\omega_l+k(\omega_u-\omega_l)/N$ means the discrete frequency; X_k and Y_k are the orthogonal random variables, which can be defined as a random function with one elementary random variable γ as follows

$$X_k=\sqrt{2}\cos(k\gamma+\pi/4),\quad X_k=\sqrt{2}\sin(k\gamma+\pi/4) \quad (4)$$

in which the elementary random variable γ is uniformly distributed within $[-\pi, \pi]$.

In Eq. (3), a modified K-T (Kanai-Tajimi) spectrum with high-pass filter modulated by a random variable based envelope function in Yang and Zhou (2015) is used to express the nonstationary spectral function, namely

$$S(t,\omega)=\left|e(t)\right|^2G(\omega)S_{\mathrm{K\text{-}T}}(\omega) \quad (5)$$

where $e(t)$, $G(\omega)$ and $S_{\mathrm{K\text{-}T}}(\omega)$ indicate the envelope function, Butterworth filter, K-T spectrum, respectively. To present the variability of envelope function, the following stochastic envelope function with three random parameters (Yang and Zhou 2015) is also adopted

$$S_{\text{K-T}}(\omega)=\frac{1+4\xi_g^2\,\omega^2/\omega_g^2}{\left(1-\omega^2/\omega_g^2\right)^2+4\xi_g^2\,\omega^2/\omega_g^2}S_0$$
$$G(\omega)=\frac{\omega^{2N}}{\omega^{2N}+\omega_h^{2N}} \tag{6}$$

$$e(\alpha,\beta,t_{pk};t)=\begin{cases}0 & t\le t_0\\ \left(\dfrac{t-t_0}{t_{pk}}\right)^{\alpha} & t_0\le t\le t_0+t_{pk}\\ e^{-\beta(t-t_0-\tau)} & t\ge t_0+t_{pk}\end{cases} \tag{7}$$

In Eq. (7) the parameter t_0 describes the initial instant of non-zero ground motion; t_{pk} denotes the time of peak value of residual acceleration; α and β are the power exponents corresponding to the ascending and descending segments. In this model, the envelope parameters t_{pk}, α and β are considered as random variables.

Consequently, the stochastic velocity time history $V_s(t)$ of ground motion scaled by the peak of residual velocity history V_{res}, and the high-frequency acceleration $a_s(t)$ of the near-fault ground motion can then be obtained by differentiating the scaled velocity time series. Finally, the acceleration time series with the strongest pulse can be generated by the superposition of the high-frequency acceleration and the low-frequency counterpart $a_p(t)$ achieved from the velocity pulse function shown in Eq. (1).

3. PARAMETERS ESTIMATION AND SYNTHESIS OF GROUND MOTIONS

3.1 Model parameters identification

As stated in Section 2.1, the velocity time history with strongest velocity pulse is first generated based on the two orthogonal components of fault-normal and fault-parallel directions by means of wavelet transformation. Then, the long-period velocity pulse time history can be extracted from the generated velocity time history with strongest pulse by utilizing a low pass filter. Finally, the pulse parameters in Eq. (1) can be identified by the nonlinear least square method:

$$(\hat{T}_p,\hat{N}_c,\hat{T}_{pk},\hat{\varphi},\hat{\sigma}_{\ln PGV})=\arg\min\sum_{i=1}^{N_t}\left[v(t_i)-v_p(t_i;T_p,N_c,T_{pk},\varphi,\sigma_{\ln PGV})\right]^2 \tag{8}$$

To identify the parameters of envelop function, the instantaneous amplitude $\tilde{a}(t)$ of residual acceleration time histories $\ddot{x}(t)$ are first solved by combining with its Hilbert transformation $\ddot{x}_H(t)$, i.e.,

$$\tilde{a}(t)=\sqrt{\ddot{x}(t)^2+\ddot{x}_H(t)^2} \tag{9}$$

Then, the multimodal point method is adopted to find the local maximal value of instantaneous amplitude in Eq. (9) so as to form the pth level envelope $\widehat{a}^{(p)}(t)$. Then, the obtained envelope $\widehat{a}^{(p)}(t)$ is fitted by envelope function $e(t)$ in Eq. (7) to identify the envelope parameters in a least square sense:

$$(\hat{t}_{pk},\hat{\alpha},\hat{\beta})=\arg\min\sum_{i=1}^{N_t}\left[\widehat{a}^{(p)}(t_i)-e(t_i;t_{pk},\alpha,\beta)\right]^2 \tag{10}$$

Figure 1 shows the 2th envelope lines of residual acceleration time history recorded at station TCU031.

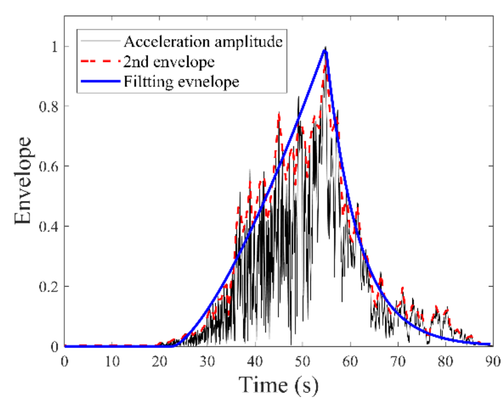

Figure 1: Envelope of the acceleration time history with strongest pulse at TCU031 station

In this study, the model parameters are identified by 34 near-fault pulse-like records with the rupture forward directivity effect in the range of fault distance $R_{\mathrm{rup}} \leqslant 30$ km in Chichi earthquake event (M_w=7.6). Table 1 shows the probability distribution of model parameters and its mean value and standard deviation, in which model parameter for high frequency γ is uniformly distributed within [−π, π] to represent the residual high-frequency stochastic process.

Table 1: Probability distribution of parameters of stochastic ground motion model

Parameters	Distribution	Bounds	Mean	Std. D.
T_p	Normal	[2.39, 10.84]	6.72	1.89
N_c	Lognormal	[1.10, 4.23]	2.35	0.74
T_{pk}	Normal	[7.04, 51.60]	25.69	10.05
φ	Uniform	[0, 2π]	2.32	1.95
$\sigma_{\ln PGV}$	Normal	[−0.6, 0.6]	0.00	0.25
t_{pk}	Normal	[10.43,47.58]	25.63	9.18
α	Lognormal	[0.22, 14.14]	2.59	3.34
β	Lognormal	[0.03, 0.41]	0.09	0.07
γ	Uniform	[−π, π]	0.00	$\pi^2/3$

3.2 Synthesis of near-fault pulse-like ground motions

After obtaining the probability distribution of model parameters, the representative ground motions can be generated by means of the point selection technology (Liu et al. 2016, Li and Chen 2009). In this work, a new point selection technique based on the generalized F-discrepancy (GF-discrepancy) (Chen et al. 2016) is adopted, which is suitable for the cases of non-normal distributed parameters.

The GF-discrepancy is defined as

$$D_{GF} = \max_{1\le i\le s}\left\{\sup\left|F_{N,i}(\theta)-F_i(\theta)\right|\right\} \qquad (11)$$

where $F_i(\theta)$ is the marginal CDF of the ith random variable; $F_{N,i}(\theta)$ is the empirical CDF considering the effects of assigned probability

$$F_{n,i}(\theta)=\sum_{q=1}^{N} P_q \cdot I\{\theta_{q,i}<\theta\} \qquad (12)$$

The first step is to generate the N initial point set $\boldsymbol{\theta}_q = (\theta_{q,1}, \theta_{q,2}, \ldots, \theta_{q,s})$, q =1, 2, …, N from a Sobol set I_n={($u_{q,1}$, $u_{q,2}$, …, $u_{q,s}$), q =1, 2, …, N} over a unit hypercube by

$$\theta_{m,i} = F_i^{-1}(u_{m,i}) \qquad (13)$$

where $F_i^{-1}(\bullet)$ denotes the inverse CDF of the ith random variable. To ensure that the weights of numerical integration, that is, assigned probability are close to each other, then the following transformation is performed in each dimension

$$\theta'_{m,i} = F_i^{-1}\left(\sum_{q=1}^{N}\frac{1}{N}\cdot I\{\theta_{q,i}<\theta_{m,i}\}+\frac{1}{2}\cdot\frac{1}{N}\right) \qquad (14)$$

The second step is to calculate the assigned probability and transform point set so as to minimize the assigned probability of point set. Hence, the point set $\boldsymbol{\theta}'_q=(\theta'_{q,1},\theta'_{q,2},\ldots,\theta'_{q,s})$, q =1, 2, …, N are further transformed as

$$\theta''_{m,i} = F_i^{-1}\left(\sum_{q=1}^{N} P_q\cdot I\{\theta'_{q,i}<\theta'_{m,i}\}+\frac{1}{2}\cdot P_m\right) \qquad (15)$$

By using the new points selection technique, the final representation points with smaller GF-discrepancy can be determined as $\boldsymbol{\theta}''_q=(\theta''_{q,1},\theta''_{q,2},\ldots,\theta''_{q,s})$.

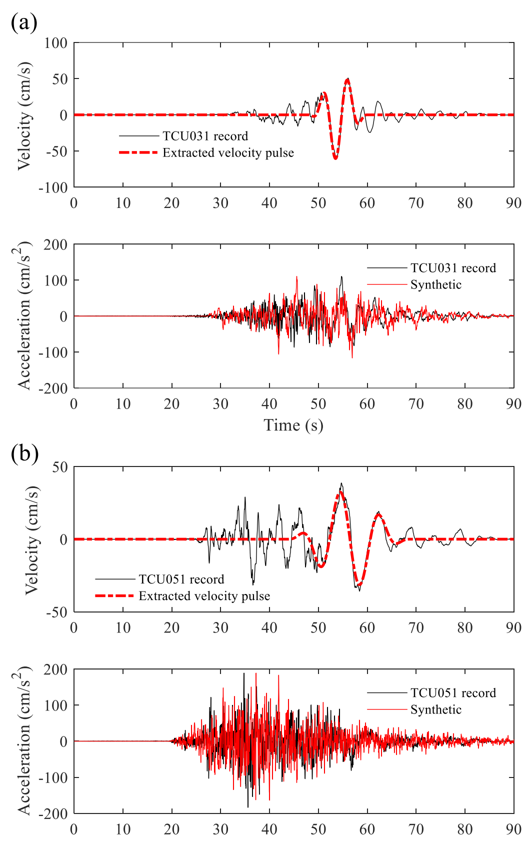

Figure 2: Velocity and acceleration time histories at the station of (a) TCU031; (b) TCU051

Figure 2 illustrates the velocity and acceleration time histories at stations of TCU031 and TCU051. From these figures, one can observe that the velocity pulses can be effectively extracted from the velocity time histories of actual records, and the synthetic acceleration time histories are matched with the original records

4. DYNAMIC RELIABILITY ASSESSMENT VIA DIRECT PROBABILITY INTEGRAL METHOD

4.1 Synthesis of near-fault pulse-like ground motions

A nonlinear MDOF system subjected to the ground motion acceleration can be descripted by the following differential motion equation (physical mapping)

$$\mathbf{M}\ddot{\mathbf{X}} + \mathbf{C}\dot{\mathbf{X}} + \mathbf{f}(\mathbf{X}) = -\mathbf{MI}\ddot{u}_g(\Theta, t) \qquad (16)$$

with the deterministic initial condition

$$\mathbf{X}(t)\big|_{t=0} = \mathbf{X}_0, \quad \dot{\mathbf{X}}(t)\big|_{t=0} = \dot{\mathbf{X}}_0 \qquad (17)$$

where $\mathbf{X}$ represents the relative displacement vector; $\mathbf{M}$ and $\mathbf{C}$ are mass and damping matrix, respectively; $\mathbf{f}$ indicates the restoring force vector; $\mathbf{I}$ is the n×1 unit column vector; $\ddot{u}_g(\mathbf{\Theta},t)$ is the acceleration history of near-fault impulsive ground motion descripted in Section 3; $\mathbf{\Theta}=(T_p, N_c, T_{\mathrm{pk}}, \varphi, \sigma_{\mathrm{lnPGV}}, \alpha, \beta, t_{\mathrm{pk}}, \gamma)$ denotes the random parameters vector of near-fault ground motion; the deterministic initial condition $\mathbf{X}_0$ and $\dot{\mathbf{X}}_0$ are considered in this study.

Based on the principle of probability conservation of random event description, Chen and Yang 0 derived uniformly the probability density integral equations (PDIEs) for static and dynamic structural systems, respectively. In this study, the structure is subjected to the seismic ground motions. The PDIE of dynamic version, therefore, is expressed as follows

$$p_{\mathrm{X}}(\mathbf{x},t) = \int_{\Omega_{\mathbf{\Theta}}} p_{\mathbf{\Theta}}(\boldsymbol{\theta})\delta\left[\mathbf{x} - \mathbf{g}(\boldsymbol{\theta},t)\right]\mathrm{d}\boldsymbol{\theta} \qquad (18)$$

where $\delta(\cdot)$ is the Dirac delta function; $\mathbf{g}(\boldsymbol{\theta},t)$ denotes the solution of physical equation in Eq. (17); $p_{\mathbf{\Theta}}(\boldsymbol{\theta})$ is the joint probability density function of random parameters $\mathbf{\Theta}$; $\Omega_{\mathbf{\Theta}}$ is the distribution domain of $\mathbf{\Theta}$.

If the certain component of responses $X(t)$ is concerned, the PDIE in Eq. (18) can be reduced according to the property of Dirac delta function, that is

$$p_X(x,t) = \int_{\Omega_{\mathbf{\Theta}}} p_{\mathbf{\Theta}}(\boldsymbol{\theta})\delta\left[x - g(\boldsymbol{\theta},t)\right]\mathrm{d}\boldsymbol{\theta} \qquad (19)$$

4.2 Direct probability integral method (DPIM)

To solve the PDIE in Eq. (19), the direct probability integral method (DPIM) was proposed by means of the partition of probability space and smoothing of Dirac delta function in previous work (Chen and Yang 2019, 2021).

By using the partition of probability space, the representative point set can be generated according GF-discrepancy based point selection method, then the representative ground motions can be synthesized. The PDIE in Eq. (19), therefore, can be written as (Chen and Yang 2019)

$$p_X(x,t) \simeq \sum_{q=1}^{N}\left\{\delta\left[x - g(\boldsymbol{\theta}_q,t)\right]P_q\right\} \qquad (20)$$

where the assigned probability of a representative point $\boldsymbol{\theta}_q$ is obtained by numerically solving the following integration

$$P_q = \int_{\Omega_{\mathbf{\Theta},q}} p_{\mathbf{\Theta}}(\boldsymbol{\theta})\,\mathrm{d}\,\boldsymbol{\theta} \qquad (21)$$

In numerical integration, the non-smooth Dirac delta function involved in Eq. (19) needs to be approximated by using smooth function. The previous work showed that the Gaussian function is an appropriate to treat this problem. Consequently, Eq. (20) can be further expressed as follows (Chen and Yang 2019, 2021)

$$p_X(x,t) \simeq \sum_{q=1}^{N}\left\{\frac{1}{\sqrt{2\pi}\sigma}\mathrm{e}^{-\left[x-\mathrm{g}(\boldsymbol{\theta}_q,t)\right]^2/2\sigma^2}P_q\right\} \qquad (22)$$

in which σ is the smoothing parameters. When $\sigma\to 0$, the smooth function $\hat{\delta}(y;\sigma)$ tends to Dirac delta function, i.e., $\delta(y) = \lim_{\sigma\to 0}\hat{\delta}(y;\sigma)$.

4.3 First-passage dynamic reliability analysis based on DPIM

Based on the first passage failure criterion, the dynamic reliability of structures is defined as (Li and Chen 2009)

$$P_{\mathrm{r}}(t)=\Pr\left\{X(\tau)\in\Omega_s, 0<\tau\le t\right\} \tag{23}$$

where Ω_s denotes the safety domain.

Accordingly, once the response crosses the safety boundary in certain moment, the system would be failure. Thus, a random process can be viewed a serial system over the time domain, namely, the structure fails when the maximum of response in time interval (0, t] exceeds the threshold. Then, the reliability of structure at instant t can be expressed as (Li and Chen 2009)

$$P_r(t)=\Pr\left\{\bigcap_{0<\tau\le t} X(\mathbf{\Theta},\tau)\in\Omega_s\right\}=\Pr\left\{X_{\max}<b\right\} \tag{24}$$

where b is the given threshold; $X_{\max}=h(\mathbf{\Theta})=\max\limits_{0<\tau\le t}\left\{\left|X(\mathbf{\Theta},\tau)\right|\right\}$, which is a mapping $\mathcal{H}$: $\mathbf{\Theta}\rightarrow X_{\max}$. The stochastic response $Y(t)$ is transformed into the random variable $X_{\max}$, then the performance can be rewritten as follows

$$Z=g(\mathbf{\theta})=b-h(\mathbf{\theta}) \tag{25}$$

In the context of the DPIM, the PDF of performance in Eq. (25) can be attained by

$$p_Z(z)\simeq\sum_{q=1}^{N}\left\{\frac{1}{\sqrt{2\pi}\sigma}\mathrm{e}^{-[z-g(\mathbf{\theta})]^2/2\sigma^2}P_q\right\} \tag{26}$$

Thus, the dynamic reliability at instant t can also be calculated by

$$P_r(t)=\Pr[Z>0]=\int_0^{\infty}p_Z(z)\,\mathrm{d}z \tag{27}$$

This approach transforms the stochastic process into a random variable to obtain the dynamic reliability of structures.

5 NUMERICAL EXAMPLE

In this section, a two-span 20-story shear frame subjected to stochastic ground motion, as illustrated in Fig. 3, is considered. The floor lumped masses of the frame are from the bottom to top floor are taken as: $m_1=m_2=4.5$, $m_3=\ldots=m_{12}=4.3$, $m_{13}=\ldots=m_{17}=4.1$, $m_{18}=m_{20}=3.9$ (10^5 kg); and the initial lateral inter-story stiffnesses: $k_1=k_2=3.5$, $k_3=\ldots=k_{12}=3.2$, $k_{13}=\ldots=k_{17}=3.0$, $k_{18}=k_{20}=2.8$ (10^8 N/m).

Assume that the failure occurs once the inter-story drift exceeds prescribed threshold, i.e., b=0.06 m. The stochastic inter-story drift is denoted as $\mathbf{Y}(\mathbf{\Theta},t)=[Y_1(\mathbf{\Theta},t), Y_2(\mathbf{\Theta},t), \ldots Y_{20}(\mathbf{\Theta},t)]$, in which $Y_1(\mathbf{\Theta},t)=X_1(\mathbf{\Theta},t)$; $Y_i(\mathbf{\Theta},t)=X_i(\mathbf{\Theta},t)-X_{i-1}(\mathbf{\Theta},t)$, $i=2,\ldots,20$. Therefore, the performance function can also be given by the mapping

$$Z=g(\mathbf{\Theta},t)=b-\max_{1\le i\le 20}\{Y_i(\mathbf{\Theta},t)\} \tag{28}$$

where the $X_i(\mathbf{\Theta},t)$ indicate the ith floor displacement of the frame, which can be calculated by the physical mapping:

$$\mathbf{M}\ddot{\mathbf{X}}+\mathbf{C}\dot{\mathbf{X}}+\alpha\mathbf{K}\mathbf{X}+(1-\alpha)\mathbf{K}\mathbf{Z}_h=-\mathbf{M}\mathbf{I}\ddot{x}(\mathbf{\Theta},t) \tag{29}$$

in which $\mathbf{M}=\mathrm{diag}(m_1, m_2,\ldots, m_{20})$ denotes the mass matrix; $\mathbf{K}$ is the initial stiffness matrix; $\mathbf{C}=\alpha_1\mathbf{M}+\alpha_2\mathbf{K}$ ($\alpha_1=0.4602$ s^{-1}, $\alpha_2=0.0041$ s) is adopted; $\mathbf{Z}_h=(Z_{h,1}, Z_{h,2}, \ldots, Z_{h,20})^{\mathrm{T}}$ denotes the hysteretic displacement, which is described by Bouc-Wen model; α is the ratio of the final tangent stiffness to initial stiffness in this model, and the other parameters are be found in Refs. (Chen and Yang 2019, 2021)

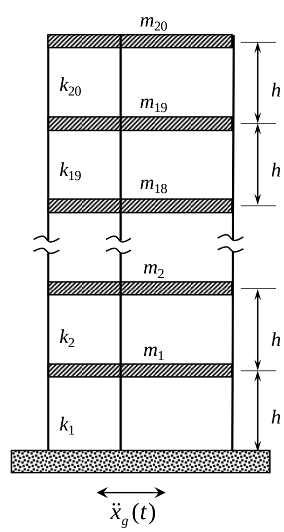

Figure 3: Two-span 20-story shear frame subjected to earthquake ground motion

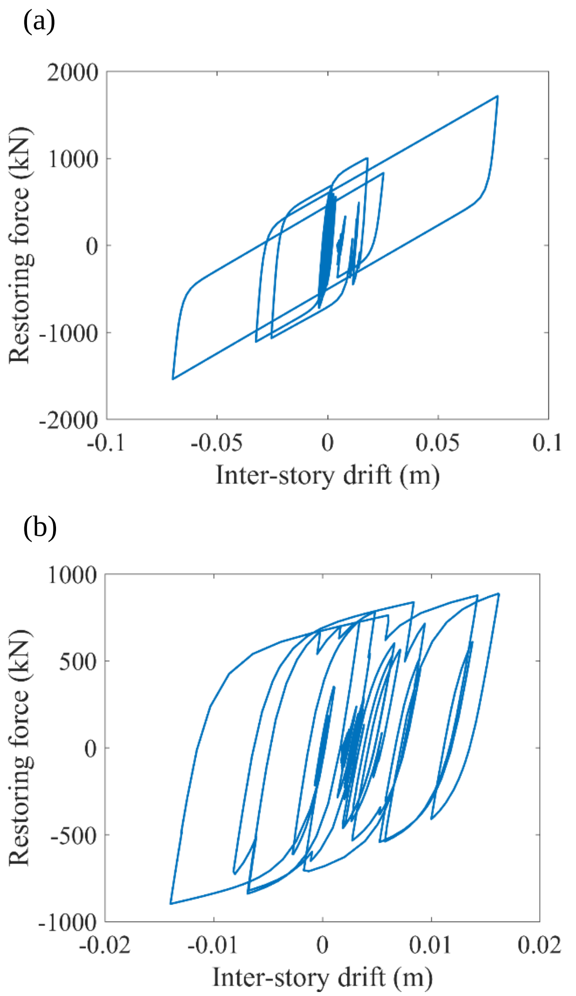

Figure 4: Restoring curves of structure under (a) pulse-like ground motion; (b) non-pulse ground motion

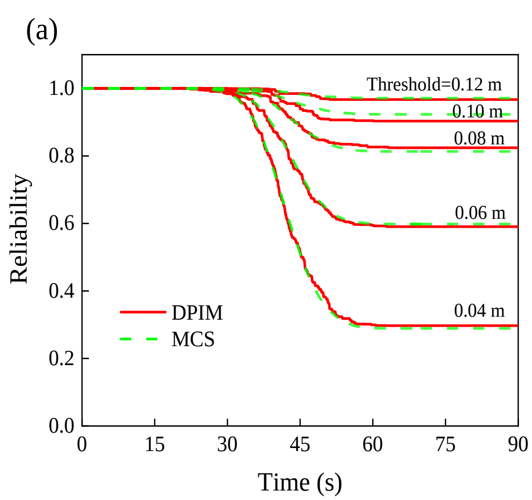

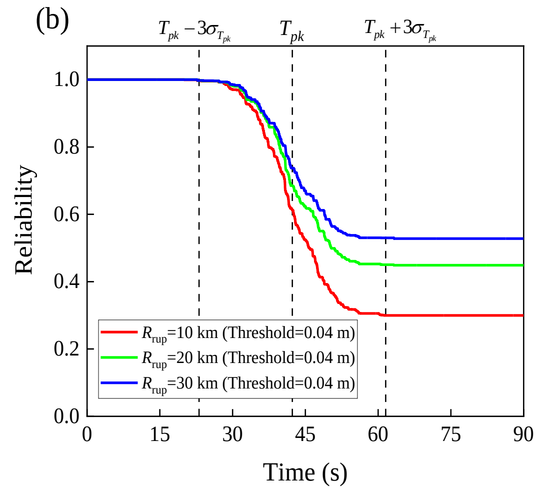

Figure 5: Dynamic reliability under different (a) thresholds and (b) fault distances R_{rup}

Figure 4 (a) and (b) illustrate the curves of restoring force versus inter-story drift of the structure subjected to near-fault pulse-like and non-pulse-like ground motion, respectively. It is seen that the velocity pulse can result in larger inter-story drift than the non-pulse like ground motion. It presents the importance of the study on reliability of structures under near-fault pulse-like ground motions.

The dynamic reliability of tall building under different threshold values (0.04, 0.06, 0.08, 0.10, 0.12 m) are depicted in Fig. 5(a). From this figure, it shows that the DPIM obtains agree results with those by MCS, and demonstrates the good accuracy of proposed method. Fig. 5(b) examines the effect of occurrence instant T_{pk} of velocity pulse for near-fault ground motion with different fault distances on dynamic reliability of the structure. It is observed that the reliability decreases remarkably from 1 to the minimum value in the time interval $[T_{pk}-3\sigma_{T_{pk}}, T_{pk}+3\sigma_{T_{pk}}]$, and the velocity pulse of near-fault ground motion affects significantly the dynamic reliability of structures, especially for the structures located in the area closer to the fault.

6. CONCLUSIONS

In this work, an efficient framework is proposed to assess the dynamic reliability of structures subjected to near-fault pulse-like ground motions.

Firstly, a stochastic synthesis model is established on the basis of near-fault ground motion records. Then, the direct probability integral method is employed to perform dynamic reliability analysis for nonlinear structures. As a numerical example, the dynamic reliability of the 20-story shear frame building is achieved.

Accordingly, the velocity pulse of near-fault ground motion has a critical effect on failure of structures in the area closer to the rupturing fault. The variability of velocity pulse parameters plays an important role and cannot be neglected in structural dynamic reliability analysis. The proposed DPIM is an efficient and accurate method for dynamic reliability assessment of nonlinear structure subjected to near-fault pulse-like ground motions.

ACKNOWLEDGMENTS

The supports of the National Natural Science Foundation of China (Grant Nos. 12102080, 12032008) are much appreciated.

7. REFERENCES

Baker, J.W. (2007). "Quantitative Classification of Near-fault Ground Motions Using Wavelet Analysis". *Bulletin of the Seismological Society of America*, 97(5), 1486−1501.

Bray, J.D., and Rodriguez-Marek A. (2004). "Characterization of Forward-directivity Ground Motions in the Near-fault Region". *Soil Dynamics and Earthquake Engineering*, 24(11), 815−828.

Chen, G.H., and Yang, D.X. (2019). "Direct probability integral method for stochastic response analysis of static and dynamic structural systems". *Computer Methods in Applied Mechanics and Engineering*, 357:112612.

Chen, G.H., and Yang D.X. (2021). "A unified analysis framework of static and dynamic structural reliabilities based on direct probability integral method". *Mechanical Systems and Signal Processing*, 158:107783

Chen, G.H., Yang, D.X., Liu Y.H., and Guo H.C. (2022). "System reliability analysis of static and dynamic structures via direct probability integral method". *Computer Methods in Applied Mechanics and Engineering*, 388: 114262.

Chen, J.B., Yang, J.Y., and Li, J. (2016). "A GF-discrepancy for point selection in stochastic seismic response analysis of structures with uncertain parameters". *Structural Safety*, 59, 20−31.

Dabaghi, M., and Der Kiureghian, A. (2017). "Stochastic Model for Simulation of Near-fault Ground Motions". *Earthquake Engineering & Structural Dynamics*, 46(6), 963−984.

Dickinson, B.W., and Gavin, H.P. (2011). "Parametric Statistical Generalization of Uniform-hazard Earthquake Ground Motions". *Journal of Structural Engineering*, 137(3), 410−422.

Li, J., and Chen, J.B. (2009). "*Stochastic Dynamics of Structures*", Singapore, John Wiley & Sons.

Liu, Z.J., Liu, W., and Peng, Y.B. (2016). "Random Function based Spectral Representation of Stationary and Non-stationary Stochastic Processes". *Probabilistic Engineering Mechanics*, 45, 115−126.

Mavroeidis, G.P., and Papageorgiou A.S. (2003). "A Mathematical Representation of Near-fault Ground Motions". *Bulletin of the Seismological Society of America*, 93(3), 1099−1131.

Melchers, R.E., and Beck, A.T. (2018). "*Structural Reliability Analysis and Prediction"*, John Wiley & Sons.

Yang, D.X., and Zhou J.L. (2015). "A Stochastic Model and Synthesis for Near-fault Impulsive Ground Motions". *Earthquake Engineering & Structural Dynamics*, 44(2), 243−264.